

Observability transition in multiplex networks

Saeed Osat¹ and Filippo Radicchi²

¹*Molecular Simulation Laboratory, Department of Physics, Faculty of Basic Sciences, Azarbaijan Shahid Madani University, Tabriz 53714-161, Iran*

²*Center for Complex Networks and Systems Research, School of Informatics and Computing, Indiana University, Bloomington, Indiana 47408, USA**

We extend the observability model to multiplex networks. We present mathematical frameworks, valid under the treelike ansatz, able to describe the emergence of the macroscopic cluster of mutually observable nodes in both synthetic and real-world multiplex networks. We show that the observability transition in synthetic multiplex networks is discontinuous. In real-world multiplex networks instead, edge overlap among layers is responsible for the disappearance of any sign of abruptness in the emergence of the the macroscopic cluster of mutually observable nodes.

I. INTRODUCTION

Complex systems where elementary units have different types of interactions can be conveniently modelled as multiplex networks [1–3]. This is a very generic representation, where elements of a system are organized in multiple network layers, each standing for a specific color or flavour of interaction. Systems that can be represented in this way are abundant in the real world. Examples include, among others, social networks sharing the same actors [4, 5], and multimodal transportation graphs sharing common geographical locations [6, 7].

Several analyses of multiplex networks have been performed recently [1–3]. A common result, shared by the vast majority of these studies, is that a processes defined on a multiplex network is characterized by features radically different from those observed for the same type of process when this is applied to an isolated network. Examples regard dynamical processes taking place on multiplex networks, such as diffusion [8, 9], epidemic spreading [10–13], synchronization [14], and controllability [15]. Examples include also structural processes as those typically framed in terms of percolation models. For instance in their seminal paper, Buldyrev *et al.* considered a site-percolation model aimed at understanding the role of interdependencies among two network layers [16]. The macroscopic cluster of mutually connected nodes in a multiplex network emerges discontinuously, at odds with what instead observed for the same process on an isolated network where the percolation transition is always continuous. A large number of subsequent studies have then analyzed in detail the features of the percolation transition in multiplex networks [17–28]. Several variants of the percolation model have been also considered, including redundant site percolation [29], k-core percolation [30], weak percolation [31], and bond percolation [32].

In this paper, we focus our attention on an additional variant of the percolation model usually named as the observability model [33, 34]. In isolated networks, the

model finds its motivation in the study of some dynamical processes where the state of the system can be determined by monitoring or dominating the states of a limited number of nodes in the network [35]. Examples include, among others, real-time monitoring of power-grid networks [33] and mobile ad-hoc networks [36]. The observability model has been considered in synthetic models [33] and real-world topologies [34]. In the simplest version of the model, every node in the network can host an observer with probability ϕ . Placing an observer on one node can make the node itself and all its nearest neighbors observable. Nodes in the network can therefore assume three different states: (i) directly observable, if hosting an observer; (ii) indirectly observable, if being the first neighbor of an observer; (iii) or not observable, otherwise. Observable, either directly or indirectly, nearest-neighbor nodes form clusters of connected observable nodes. As in the case of percolation, the question of interest in network observability is understanding the macroscopic formation of observable clusters in the network on the basis of microscopic changes in the state of its individual nodes. In synthetic infinite graphs, the macroscopic cluster of observable nodes obeys a continuous phase transition as a function of the probability ϕ , and the critical threshold is generally very small [33]. In most real-world networks also, the largest cluster grows smoothly, and the transition point is generally very close to zero [34].

In our extension of the observability model to multiplex networks, we focus our attention on the emergence of clusters of mutually observable nodes. The definition of these clusters is a straightforward combination of the notions of clusters of observable nodes in isolated networks [33] and clusters of mutually connected nodes in multiplex networks [16]. The extension of the observability model to multiplex networks finds its rationale in any situation where the goal is monitoring or controlling the dynamics of a system structured in multiple layers of interactions. A genuine example could be tracking the spread of information on two coupled social media, such as Facebook and Twitter. Actors are shared by the two social networks. Observing an individual means getting full access to her/his accounts thus being able to read the

*Electronic address: filiradi@indiana.edu

content of the messages that the individual, and her/his friends, are posting on the two platforms. Clusters of mutually observable nodes in this sense correspond to connected portions of the systems where the content of information that is exchanged by people within the cluster can be completely monitored.

The paper is organized as follows. In section II, we define the observability model in multiplex networks. In section III, we study the model in ensembles of multiplex networks whose layers are generated according to the configuration model. In section IV, we introduce a message-passing method to deal with the observability model in multiplex networks with specified topology, such as real-world multiplex networks. The framework described in this section is based on the assumption that the number of edges shared by the different layers of the multiplex is negligible. The message-passing method valid for multiplex networks in presence of edge overlap is much more cumbersome, and, for this reason, presented only in the Supplemental Material. Finally, in section V, we summarize the main findings of the paper.

II. OBSERVABILITY MODEL IN MULTIPLEX NETWORKS

We consider a multiplex network composed of N nodes structured in two layers, namely α and β . Node labels take integer values from 1 to N in both layers. Nodes with identical labels correspond to copies (or replicas) of the same individual or unit in the two layers. The observability model we consider here is a natural extension to multiplex networks of the same model already considered on isolated networks [33, 34]. Observers or sensors are placed at random with probability ϕ on every node in the system. If an observer is placed on a node i , the node i is directly observable in both layers. A node i , that is not directly observable, but is attached to at least one directly observable node j in layer α and at least one directly observable node k in layer β , with j not necessarily equal to k , is indirectly observable. We focus our attention on mutually observable clusters of nodes. The way these clusters are defined is identical to the one in which clusters of mutually connected nodes are defined in site percolation [16]. The only difference comes from the fact that a node in order to be ‘‘occupied’’ can be either in the directly or indirectly observable state. Note that mutually connected and mutually observable clusters coincide for $\phi = 1$. In particular, a cluster of mutually observable nodes is defined in a recursive manner and is composed by all the nodes that are connected by at least by one path (internal to the cluster itself) in both layers. Our model can be seen as a depth-one percolation model on a multiplex network. As we are interested in understanding the extent of the system that can be monitored by placing random points of observation, the focus of our analysis is centered on quantifying how the size of the Largest Mutually Observable Cluster (LMOC)

changes as a function of the microscopic probability ϕ of nodes to be directly observable. To generate the mathematical framework necessary to study such a model, we make use of a simple self-consistent condition: an observable node belongs to the LMOC if it has, in both layers, at least one neighbor that is part of the LMOC. Such a condition can be expressed in terms of elementary conditional probabilities defined for the edges and the nodes of the multiplex network. In the following, we discuss the details of how the mathematical framework can be solved exactly under two conditions: (i) absence of link overlap among layers, and (ii) validity of the locally tree-like ansatz. In the Supplemental Material, we report the full mathematical framework valid when condition (i) is removed.

III. OBSERVABILITY TRANSITION IN RANDOM MULTIPLEX NETWORKS

Let us consider the case of a multiplex composed of two network layers generated independently according to the configuration model [37]. If the layers are sufficiently sparse, the fact that the layers are generated independently allow us to consider the overlap among layers (i.e., the simultaneous existence of the same edge in both layers happens with vanishing probability) negligible. The only inputs required to study such a system are the degree distributions of the two layers, namely $P^{[\alpha]}(k)$ and $P^{[\beta]}(k)$.

The analytic treatment for this special types of networks is similar to one presented in Ref. [33] for isolated networks. To generate a self-consistent set of equations able to describe how the LMOC changes as a function of ϕ in this special type of multiplex networks, we define the following conditional probabilities valid for a randomly selected edge in layer α :

1. $u^{[\alpha]}$, that is the probability that one of the nodes at the end of the edge is in the LMOC given that the other node at the end of the edge is directly observable.
2. $v^{[\alpha]}$, that is the probability that one of the nodes at the end of the edge is in the LMOC given that the node at the other end of the edge is not directly observable.
3. $z^{[\alpha]}$, that is the probability that one of the nodes at the end of the edge is in the LMOC given that both nodes at the end of the edge are not directly observable.

The same exact definitions are valid for the conditional probabilities $u^{[\beta]}$, $v^{[\beta]}$, and $z^{[\beta]}$ for layer β .

As mentioned above, a generic node is part of the LMOC if observable, either directly or indirectly, and attached to at least one other node that is part of the LMOC. The way this happens depends however on the

state of the node. We make therefore a distinction between (i) a directly observable node and (ii) a not directly observable node.

Let us consider first case (i). If one of the nodes at the end of a generic edge is directly observable, the probability that the node is not connected to the LMOC is $\phi(1 - u^{[\alpha]})$ if the other node is directly observable, or $(1 - \phi)(1 - v^{[\alpha]})$ if the other node is not directly observable. If the node we are considering has degree k , then then probability that the node is connected to the LMOC in layer α is

$$q_k^{[\alpha]} = 1 - \sum_{m=0}^k \binom{k}{m} [\phi(1 - u^{[\alpha]})]^m [(1 - \phi)(1 - v^{[\alpha]})]^{k-m} .$$

The sum on the r.h.s. of the equation above quantifies the probability for the none of the neighbors of a node with degree k is part of the LMOC. This probability is then discounted from 1 to estimate the probability that at least one neighbor of the node is part of the LMOC. If we consider all nodes, we have that

$$q^{[\alpha]} = \sum_k P^{[\alpha]}(k) q_k^{[\alpha]} = 1 - G_0^{[\alpha]} \left(1 - \phi u^{[\alpha]} - (1 - \phi) v^{[\alpha]} \right) ,$$

where $G_0^{[\alpha]}(x) = \sum_k P^{[\alpha]}(k) x^k$ is the generating function of the degree distribution for layer α . We can repeat the same exact arguments for layer β . In particular, the probability that a generic node is part of the LMOC is given by the product that the node is attached to the LMOC simultaneously in both layers, that is

$$q = \phi q^{[\alpha]} q^{[\beta]} , \quad (1)$$

where the extra factor ϕ comes from the fact that we are considering the case of a node that is directly observable.

For case (ii), we can proceed in a similar way as above. If our node is not directly observable, and we select one of its edges at random, then the probability that this node is not connected to the LMOC is $\phi(1 - u^{[\alpha]})$ if the other node at the end of the edge is directly observable, or $(1 - \phi)(1 - z^{[\alpha]})$ if the other node is not directly observable. If the node we are considering has degree k , the probability that this node is connected to the LMOC in layer α is

$$r_k^{[\alpha]} = 1 - (1 - \phi)^k + \sum_{m=1}^k \binom{k}{m} [\phi(1 - u^{[\alpha]})]^m [(1 - \phi)(1 - z^{[\alpha]})]^{k-m} .$$

The term $(1 - \phi)^k$ comes from the fact that if none of the nodes at the end of the k edges departing from our node are directly observable, then necessarily our node will be not indirectly observable and thus surely out of any cluster. The remaining part of the r.h.s. instead quantifies the probability that none of the neighbors of our node is part of the LMOC, assuming that at least one of them is directly observable. Both these probabilities are discounted from 1 to compute the probability that

our indirectly observable node is part of the LMOC. If we consider all nodes, we have that

$$r^{[\alpha]} = \sum_k P^{[\alpha]}(k) r_k^{[\alpha]} = 1 - G_0^{[\alpha]} \left(1 - \phi u^{[\alpha]} - (1 - \phi) z^{[\alpha]} \right) + G_0^{[\alpha]} \left((1 - \phi)(1 - z^{[\alpha]}) \right) - G_0^{[\alpha]} (1 - \phi) .$$

For layer β , the arguments are identical. The probability that a generic node that is not directly observable is part of the LMOC is given by the product that the node is attached to the LMOC simultaneously in both layers, that is

$$r = (1 - \phi) r^{[\alpha]} r^{[\beta]} , \quad (2)$$

where the extra factor $1 - \phi$ comes from the fact that we are considering the case of a node that is not directly observable. Combining cases (i) and (ii) together, we can finally write

$$P_\infty = q + r , \quad (3)$$

for the average size of the LMOC. To compute Eq. (3), we still require a way to estimate properly the conditional probabilities $u^{[\alpha]}$, $u^{[\beta]}$, $v^{[\alpha]}$, $v^{[\beta]}$, $z^{[\alpha]}$, and $z^{[\beta]}$. Following a similar approach as the one described above, we have that

$$u^{[\alpha]} = \frac{[1 - G_1^{[\alpha]}(1 - \phi u^{[\alpha]} - (1 - \phi) v^{[\alpha]})] \times [1 - G_0^{[\beta]}(1 - \phi u^{[\beta]} - (1 - \phi) v^{[\beta]})]}{[1 - G_1^{[\alpha]}(1 - \phi u^{[\alpha]} - (1 - \phi) v^{[\alpha]})] \times [1 - G_0^{[\beta]}(1 - \phi u^{[\beta]} - (1 - \phi) v^{[\beta]})] + G_0^{[\beta]}(1 - \phi) + G_0^{[\beta]}((1 - \phi)(1 - z^{[\beta]})]} , \quad (4)$$

$$v^{[\alpha]} = \frac{[1 - G_1^{[\alpha]}(1 - \phi u^{[\alpha]} - (1 - \phi) z^{[\alpha]})] \times [1 - G_0^{[\beta]}(1 - \phi u^{[\beta]} - (1 - \phi) z^{[\beta]})] + G_0^{[\beta]}(1 - \phi) + G_0^{[\beta]}((1 - \phi)(1 - z^{[\beta]})]}{[1 - G_1^{[\alpha]}(1 - \phi u^{[\alpha]} - (1 - \phi) z^{[\alpha]})] \times [1 - G_0^{[\beta]}(1 - \phi u^{[\beta]} - (1 - \phi) z^{[\beta]})] + G_0^{[\beta]}(1 - \phi) + G_0^{[\beta]}((1 - \phi)(1 - z^{[\beta]})]} , \quad (5)$$

and

$$z^{[\alpha]} = \frac{[1 - G_1^{[\alpha]}(1 - \phi u^{[\alpha]} - (1 - \phi) z^{[\alpha]}) + G_1^{[\alpha]}(1 - \phi) + G_1^{[\alpha]}((1 - \phi)(1 - z^{[\alpha]})] \times [1 - G_0^{[\beta]}(1 - \phi u^{[\beta]} - (1 - \phi) z^{[\beta]})] + G_0^{[\beta]}(1 - \phi) + G_0^{[\beta]}((1 - \phi)(1 - z^{[\beta]})]}{[1 - G_1^{[\alpha]}(1 - \phi u^{[\alpha]} - (1 - \phi) z^{[\alpha]}) + G_1^{[\alpha]}(1 - \phi) + G_1^{[\alpha]}((1 - \phi)(1 - z^{[\alpha]})] \times [1 - G_0^{[\beta]}(1 - \phi u^{[\beta]} - (1 - \phi) z^{[\beta]})] + G_0^{[\beta]}(1 - \phi) + G_0^{[\beta]}((1 - \phi)(1 - z^{[\beta]})]} . \quad (6)$$

The intuition behind the previous equations is straightforward. When looking at an edge on layer α , the probability that this edge will bring to the LMOC will depend on the generating function of the excess degree distribution of the layer, i.e., $G_1^{[\alpha]}(x) = [d/dx G_0^{[\alpha]}(x)]/[d/dx G_0^{[\alpha]}(1)]$. On the other hand, the probability that a node at the end of this edge is also attached to the LMOC on layer β will depend only on the degree of the node itself on layer β , accounted by the generating function of the degree distribution, namely $G_0^{[\beta]}(x)$. Note that equations for $u^{[\beta]}$, $v^{[\beta]}$, and $z^{[\beta]}$ can be obtained by simply swapping α and β in Eqs. (4), (5), and (6).

At this point, we have everything necessary to estimate Eq. (3). We have first to solve Eqs. (4), (5), and (6), and

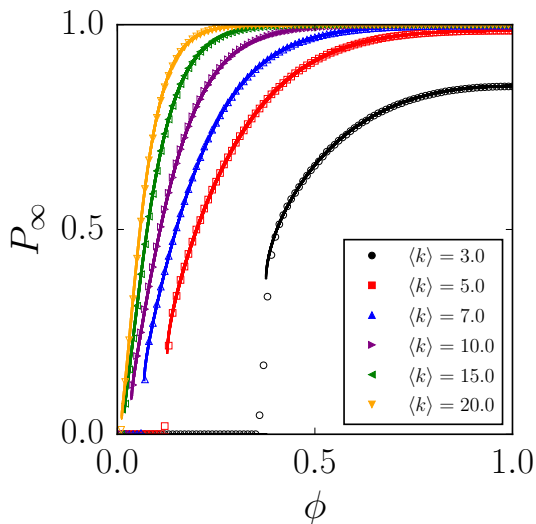


Figure 1: Observability transition in random Poisson multiplex networks. We consider multiplex networks with layers generated independently and given by realizations of the configuration model with $N = 10,000$ nodes and degree sequence generated according to a Poisson distribution with average degree $\langle k \rangle$. Results of our theoretical method (small symbols) are compared with those of numerical simulations of the observability model (large symbols). We consider different values of $\langle k \rangle$, $\langle k \rangle = 3.0, 5.0, 7.0, 10.0, 15.0$, and 20.0 . Values of P_∞ for the various cases drop to zero in the same order if the figure is read from right to left.

the analogous ones for layer β , by iteration. Then, we can plug the obtained values of the conditional probabilities for generic edges into the equations for the nodes.

Figure 1 shows a comparison between the results of direct numerical simulations of the observability model and the numerical solutions of our equations for duplex networks formed by layers obeying Poisson degree distributions, i.e., $P^{[\alpha]}(k) = P^{[\beta]}(k) = \frac{\langle k \rangle^k e^{-\langle k \rangle}}{k!}$. The figure provides evidence of a perfect agreement between theory and simulations. As the generating functions $G_0^{[\alpha]}$, $G_1^{[\alpha]}$, $G_0^{[\beta]}$, and $G_1^{[\beta]}$ can be written in a closed form for the Poisson distribution, we can also study the numerical solution of the equations for infinitely large networks (Fig. 2). No transition takes place for $\langle k \rangle < 2.4554$, i.e., the same value found for the standard percolation model [16]. This is expected from the equivalence between the observability model and the standard percolation model for $\phi = 1$. For $\langle k \rangle \geq 2.4554$, the behavior of the observability model becomes different from the one observed in site percolation. There, we have that the critical occupation probability p_c and the height of the discontinuous jump $P_\infty(p_c^+)$ decay to zero as a function of the average degree $\langle k \rangle$ as $p_c \propto P_\infty(p_c^+) \propto \langle k \rangle^{-1}$ [16]. For the observability model, we find instead that the rescaled critical threshold $\tilde{\phi}_c = \phi_c + (1 - \phi_c)[1 - (1 - \phi_c)^{\langle k \rangle}]$ doesn't decrease as $\langle k \rangle^{-1}$ as a naive mapping between the two models

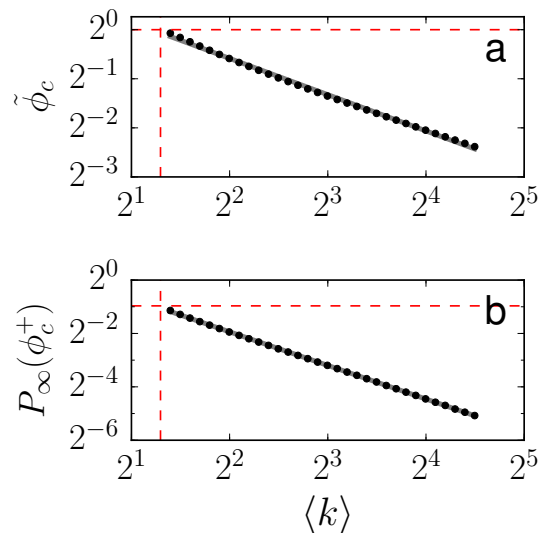


Figure 2: Observability transition in random Poisson multiplex networks. (a) We plot the rescaled value of the critical threshold $\tilde{\phi}_c = \phi_c + (1 - \phi_c)[1 - (1 - \phi_c)^{\langle k \rangle}]$ (black circles) as a function of the average degree $\langle k \rangle$ for Poisson multiplex networks of infinite size. We find that $\tilde{\phi}_c \propto \langle k \rangle^{-3/4}$ (gray full line). The vertical red line indicates the value $\langle k \rangle_c \simeq 2.4554$ where $\tilde{\phi}_c = 1$ (horizontal red line). (b) Height of the discontinuous jump $P_\infty(\phi_c^+)$ as a function of the average degree $\langle k \rangle$ (black circles) for the same multiplex networks of panel (a). We find that $P_\infty(\phi_c^+) \propto \langle k \rangle^{-7/4}$ (gray full line). The vertical red line indicates the value $\langle k \rangle_c \simeq 2.455$ where $P_\infty(\phi_c^+) \simeq 0.511$ (horizontal red line).

would predict. Instead, the scaling is compatible with $\tilde{\phi}_c \propto \langle k \rangle^{-3/4}$ (Fig. 2a). The height of the discontinuous jump $P_\infty(\phi_c^+)$ also doesn't go to zero as $\langle k \rangle^{-1}$ as predicted in the standard percolation model, but instead as $P_\infty(\phi_c^+) \propto \langle k \rangle^{-7/4}$ (Fig. 2b).

IV. OBSERVABILITY TRANSITION IN REAL MULTIPLEX NETWORKS

In this section, we develop an analytic framework able to approximate the phase diagram of the observability transition for a duplex with given adjacency matrices for the two layers. This information is encoded in the sets $\partial_i^{[\alpha]}$ and $\partial_i^{[\beta]}$ containing the neighbors of node i respectively in layers α and β for every node i . We indicate the sizes of these sets respectively as $k_i^{[\alpha]}$ and $k_i^{[\beta]}$. We make use of two assumptions: (i) layers have null overlap in the sense that set of neighbors of the same node in the two layers have null intersection; (ii) neighbors of a node are not attached to each other.

Suppose we are interested in estimating the probability s_i that node i is part of the LMOC. This will happen if node i is receiving at least one message in layer α and one message in layer β about the belonging to the LMOC.

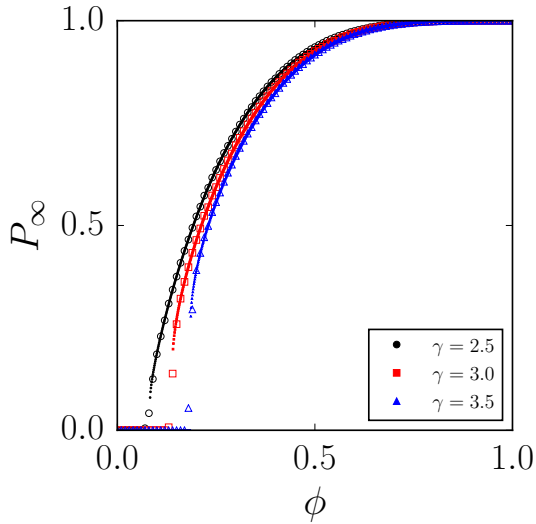


Figure 3: Observability transition in a single random scale-free multiplex networks. We consider multiplex networks with layers generated independently and given by realizations of the configuration model with $N = 10,000$ nodes and degree sequence generated according to a power-law degree distribution $P^{[\alpha]}(k) = P^{[\beta]}(k) \sim k^{-\gamma}$ with degree exponent γ (minimal degree is set $k_{min} = 3$, so that edge overlap between layers is negligible). Results of message passing framework without overlap (small symbols) are compared with those of numerical simulations of the observability model (large symbols). We consider different values of γ , $\gamma = 2.5, 3.0$ and 3.5 . Values of P_∞ for the various cases drop to zero in the same order if the figure is read from right to left.

We consider average message values over the ensemble of random placements of observers in the network. In particular, we define three different messages for every edge $j \rightarrow i$ in layer α dependent on the states of the nodes j and i :

1. $u_{j \rightarrow i}^{[\alpha]}$, that is the average value of the message that node j sends to node i , when j is directly observable.
2. $v_{j \rightarrow i}^{[\alpha]}$, that is the average value of the message that node j sends to node i , when j is not directly observable.
3. $z_{j \rightarrow i}^{[\alpha]}$, that is the average value of the message that node j sends to node i , when neither j nor i are directly observable.

$u_{j \rightarrow i}^{[\beta]}$, $v_{j \rightarrow i}^{[\beta]}$, and $z_{j \rightarrow i}^{[\beta]}$ represent the same quantities as above but for layer β . Note that messages traveling on the same edge but in opposite direction are different.

The generic node i is part of the LMOC if one of these two conditions are met: (i) the node is directly observable and attached to at least one other node in layer α and layer β that are part of the LMOC; (ii) the node is

indirectly observable and attached to at least one other node in layer α and layer β that are part of the LMOC.

Considering only layer α , for case (i), we can write

$$q_i^{[\alpha]} = \left[1 - \prod_{j \in \partial_i^{[\alpha]}} (1 - \phi u_{j \rightarrow i}^{[\alpha]} - (1 - \phi) v_{j \rightarrow i}^{[\alpha]}) \right]. \quad (7)$$

For case (ii), we have instead

$$r_i^{[\alpha]} = \left[1 - \prod_{j \in \partial_i^{[\alpha]}} (1 - \phi u_{j \rightarrow i}^{[\alpha]} - (1 - \phi) z_{j \rightarrow i}^{[\alpha]}) + (1 - \phi)^{k_i^{[\alpha]}} \left[1 - \prod_{j \in \partial_i^{[\alpha]}} (1 - z_{j \rightarrow i}^{[\alpha]}) \right] \right] \times \quad (8)$$

The same type of equations are valid for layer β . As the node must be part of the LMOC in both layer simultaneously, we can write

$$q_i = \phi q_i^{[\alpha]} q_i^{[\beta]}, \quad (9)$$

and

$$r_i = (1 - \phi) r_i^{[\alpha]} r_i^{[\beta]}, \quad (10)$$

where the factors ϕ and $1 - \phi$ come from the fact that we are considering the cases of a directly observable and a non directly observable node, respectively. The size of the average LMOC is given by

$$P_\infty = \frac{1}{N} \sum_i q_i + r_i. \quad (11)$$

The self-consistent equations for the messages are instead given by

$$u_{j \rightarrow i}^{[\alpha]} = \left[1 - \prod_{k \in \partial_j^{[\alpha]} \setminus i} (1 - \phi u_{k \rightarrow j}^{[\alpha]} - (1 - \phi) v_{k \rightarrow j}^{[\alpha]}) \right] \times \left[1 - \prod_{k \in \partial_j^{[\beta]}} (1 - \phi u_{k \rightarrow j}^{[\beta]} - (1 - \phi) v_{k \rightarrow j}^{[\beta]}) \right], \quad (12)$$

$$v_{j \rightarrow i}^{[\alpha]} = \left[1 - \prod_{k \in \partial_j^{[\alpha]} \setminus i} (1 - \phi u_{k \rightarrow j}^{[\alpha]} - (1 - \phi) z_{k \rightarrow j}^{[\alpha]}) \right] \times \left[1 - \prod_{k \in \partial_j^{[\beta]}} (1 - \phi u_{k \rightarrow j}^{[\beta]} - (1 - \phi) z_{k \rightarrow j}^{[\beta]}) + (1 - \phi)^{k_j^{[\beta]}} \left[1 - \prod_{k \in \partial_j^{[\beta]}} (1 - z_{k \rightarrow j}^{[\beta]}) \right] \right], \quad (13)$$

and

$$\begin{aligned}
z_{j \rightarrow i}^{[\alpha]} = & \left[1 - \prod_{k \in \partial_j^{[\alpha]} \setminus i} (1 - \phi u_{k \rightarrow j}^{[\alpha]} - (1 - \phi) z_{k \rightarrow j}^{[\alpha]}) + \right. \\
& \left. - (1 - \phi)^{k_j^{[\alpha]} - 1} \left[1 - \prod_{k \in \partial_j^{[\alpha]} \setminus i} (1 - z_{k \rightarrow j}^{[\alpha]}) \right] \right] \times \\
& \left[1 - \prod_{k \in \partial_j^{[\beta]}} (1 - \phi u_{k \rightarrow j}^{[\beta]} - (1 - \phi) z_{k \rightarrow j}^{[\beta]}) + \right. \\
& \left. - (1 - \phi)^{k_j^{[\beta]}} \left[1 - \prod_{k \in \partial_j^{[\beta]}} (1 - z_{k \rightarrow j}^{[\beta]}) \right] \right]
\end{aligned} \tag{14}$$

for a generic edge $j \rightarrow i$ belonging to layer α . Equations with the same structure allow to compute the probabilities defined for edges in layer β . We remark that the equations above make use of the locally treelike approximation, hence the products appearing on their right-hand sides. Further, backtracking terms are excluded in the products.

The analytic framework is now completed. To estimate the average size of the LMOC as a function of ϕ , one needs to: first, solve Eqs. (12), (13), and (14) by iteration; second, plug these solutions into Eqs. (7), and (8); third, estimate in sequence Eqs. (9), (10), and (11).

We performed comparisons between numerical solutions of the framework and results of numerical simulations for a single multiplex networks formed by random scale-free network layers which have negligible overlap (see Fig. 3). The agreement between the two approaches is remarkable.

We stress the fact that the framework presented above is valid under the assumption that the two layers that compose the multiplex do not share any edge. This is a very strong assumption, often violated by real-world networks. For instance, edge overlap may have a dramatic consequence on the properties of the percolation transition [26, 28, 38–41]. We developed a mathematical framework valid in case of edge overlap. Given its length and complexity, we present the details only in the Supplemental Material. Indeed, results from the application of the two methods (with or without edge overlap) to

real-world multiplex networks provide very different scenarios and degree of accuracy. In Figure 4 for example, we show a comparisons between numerical simulations and numerical solutions of the frameworks when applied to a multiplex transportation network [26]. The framework that accounts for edge overlap well approximates the ground-truth results obtained with numerical simulations. The observability transitions appear smooth, and the transition point is very close to zero. The framework that doesn't account for edge overlap instead shows an abrupt transition, and a threshold larger than zero. Similar considerations are valid also for the multiplex network representing the *C. Elegans* connectome (Fig. 5) [42, 43].

V. CONCLUSIONS

In this paper, we extended the observability model, originally considered on isolated networks, to multiplex networks. In particular, we focused our attention on the emergence of the largest cluster of mutually observed nodes as a function of the microscopic probability of individual nodes to host observers. We developed mathematical frameworks able to well describe the observability diagram in synthetic and real-world multiplex networks. Our results indicate that the features of this phase transition cannot be trivially deduced from those valid for the percolation transition. This statement is true both for randomly generated multiplex networks, as well as for multiplex networks representing real-world systems. Interestingly, real-world multiplex networks seem to be always in the observable regime, as long as the fraction of nodes that is directly observed is larger than zero. This fact seems due to the natural, and ubiquitously observed, presence of edge overlap among the layers that compose real multiplex networks.

Acknowledgments

FR acknowledges support from the National Science Foundation (Grant CMMI-1552487) and the US Army Research Office (W911NF-16-1-0104).

-
- [1] S. Boccaletti, G. Bianconi, R. Criado, C. I. Del Genio, J. Gómez-Gardeñes, M. Romance, I. Sendiña-Nadal, Z. Wang, and M. Zanin, *Physics Reports* **544**, 1 (2014).
 - [2] M. Kivelä, A. Arenas, M. Barthélemy, J. P. Gleeson, Y. Moreno, and M. A. Porter, *Journal of complex networks* **2**, 203 (2014).
 - [3] K.-M. Lee, B. Min, and K.-I. Goh, *The European Physical Journal B* **88**, 1 (2015).
 - [4] M. Szell, R. Lambiotte, and S. Thurner, *Proceedings of the National Academy of Sciences USA* **107**, 13636 (2010).
 - [5] P. J. Mucha, T. Richardson, K. Macon, M. A. Porter, and J.-P. Onnela, *science* **328**, 876 (2010).
 - [6] M. Barthélemy, *Physics Reports* **499**, 1 (2011).
 - [7] A. Cardillo, J. Gómez-Gardenes, M. Zanin, M. Romance, D. Papo, F. del Pozo, and S. Boccaletti, *Scientific Reports* **3**, 1344 (2013).
 - [8] S. Gómez, A. Díaz-Guilera, J. Gómez-Gardeñes, C. J. Pérez-Vicente, Y. Moreno, and A. Arenas, *Phys. Rev. Lett.* **110**, 028701 (2013).
 - [9] M. De Domenico, A. Solé-Ribalta, S. Gómez, and A. Arenas, *Proc. Natl. Acad. Sci. USA* **111**, 8351 (2014).
 - [10] M. Dickison, S. Havlin, and H. E. Stanley, *Phys. Rev. E* **85**, 066109 (2012).
 - [11] A. Saumell-Mendiola, M. A. Serrano, and M. Boguñá, *Phys. Rev. E* **86**, 026106 (2012).

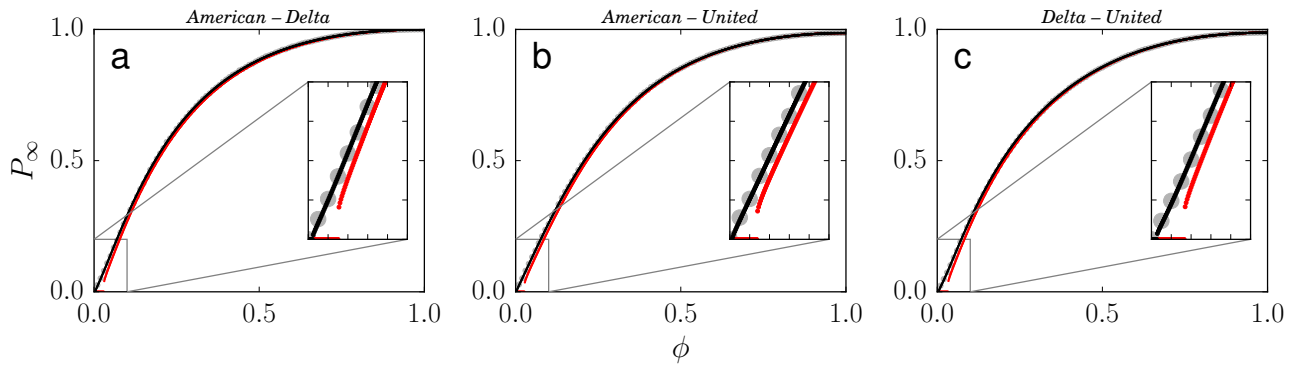


Figure 4: Observability transition in the US air transportation multiplex network. (a) The system is obtained by combining American Airlines and Delta routes. We consider only US domestic flights operated in January, 2014, and construct the duplex network where airports are nodes and connections on the layers are determined by the existence of at least a flight between the two locations. In the diagram, the gray big circles represents results of numerical simulations, the red small circles stand for results from the framework that doesn't account for edge overlap, and the black small circles represent results obtained from the mathematical framework that accounts for edge overlap. The inset shows a zoom of a specific part of the diagram. (b) Same as in panel (a), but for the combination of American Airlines and United flights. (c) Same as in panel (a), but for the combination of Delta and United flights.

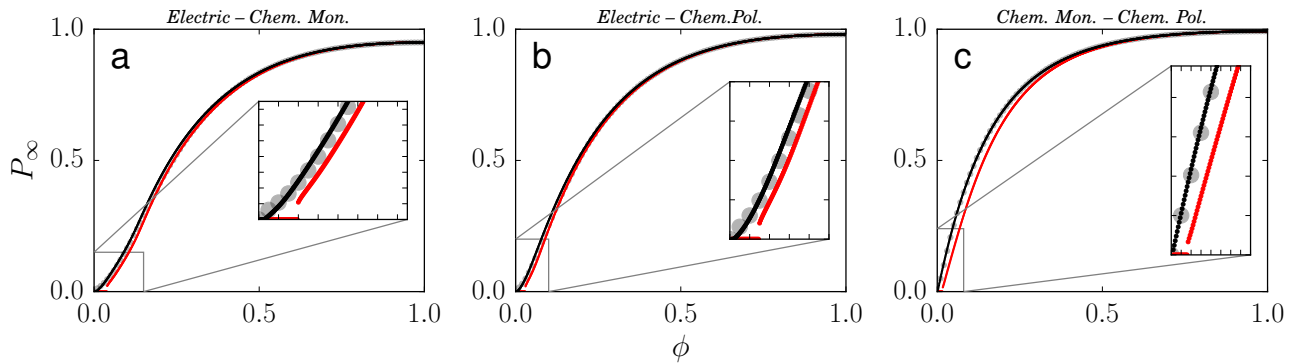


Figure 5: Observability transition in the *C. Elegans* connectome multiplex network. Edges in different layers represent different types of synaptic junctions among the neurons: electrical, chemical monadic, and chemical polyadic. (a) Analysis of the multiplex obtained by combining together the layers of electrical and chemical monadic interactions. In the diagram, the gray big circles represents results of numerical simulations, the red small circles stand for results from the framework that doesn't account for edge overlap, and the black small circles represent results obtained from the mathematical framework that accounts for edge overlap. The inset shows a zoom of a specific part of the diagram. (b) Same as in panel (a), but for the combination of electrical and chemical polyadic interactions. (c) Same as in panel (a), but for the combination of chemical monadic and polydiatic interactions.

- [12] C. Granell, S. Gómez, and A. Arenas, Phys. Rev. Lett. **111**, 128701 (2013).
- [13] M. De Domenico, C. Granell, M. A. Porter, and A. Arenas, Nature Physics (2016).
- [14] C. I. del Genio, J. Gómez-Gardeñes, I. Bonamassa, and S. Boccaletti, Science Adv. **2** (2016).
- [15] M. Pósfai, J. Gao, S. P. Cornelius, A.-L. Barabási, and R. M. D'Souza, Phys. Rev. E **94**, 032316 (2016).
- [16] S. V. Buldyrev, R. Parshani, G. Paul, H. E. Stanley, and S. Havlin, Nature **464**, 1025 (2010).
- [17] R. Parshani, S. V. Buldyrev, and S. Havlin, Physical review letters **105**, 048701 (2010).
- [18] R. Parshani, C. Rozenblat, D. Ietri, C. Ducruet, and S. Havlin, EPL (Europhysics Letters) **92**, 68002 (2011).
- [19] G. Baxter, S. Dorogovtsev, A. Goltsev, and J. Mendes, Physical review letters **109**, 248701 (2012).
- [20] S. Watanabe and Y. Kabashima, Phys. Rev. E **89**, 012808 (2014).
- [21] S.-W. Son, G. Bizhani, C. Christensen, P. Grassberger, and M. Paczuski, EPL (Europhysics Letters) **97**, 16006 (2012).
- [22] B. Min, S. Do Yi, K.-M. Lee, and K.-I. Goh, Physical Review E **89**, 042811 (2014).
- [23] G. Bianconi, S. N. Dorogovtsev, and J. F. F. Mendes, Phys. Rev. E **91**, 012804 (2015).
- [24] G. Bianconi and S. N. Dorogovtsev, Physical Review E

- 89**, 062814 (2014).
- [25] F. Radicchi and A. Arenas, *Nature Physics* **9**, 717 (2013).
 - [26] F. Radicchi, *Nature Phys.* **11**, 597 (2015).
 - [27] D. Cellai and G. Bianconi, *Physical Review E* **93**, 032302 (2016).
 - [28] G. Bianconi and F. Radicchi, *Phys. Rev. E* **94**, 060301 (2016).
 - [29] F. Radicchi and G. Bianconi, arXiv preprint arXiv:1610.05378 (2016).
 - [30] N. Azimi-Tafreshi, J. Gómez-Gardeñes, and S. N. Dorogovtsev, *Phys. Rev. E* **90**, 032816 (2014).
 - [31] G. J. Baxter, S. N. Dorogovtsev, J. F. F. Mendes, and D. Cellai, *Phys. Rev. E* **89**, 042801 (2014).
 - [32] A. Hackett, D. Cellai, S. Gómez, A. Arenas, and J. P. Gleeson, *Phys. Rev. X* **6**, 021002 (2016).
 - [33] Y. Yang, J. Wang, and A. E. Motter, *Phys. Rev. Lett.* **109**, 258701 (2012).
 - [34] Y. Yang and F. Radicchi, *Phys. Rev. E* **94**, 030301 (2016).
 - [35] Y.-Y. Liu, J.-J. Slotine, and A.-L. Barabási, *Nature* **473**, 167 (2011).
 - [36] J. Wu and H. Li, in *Proceedings of the 3rd international workshop on Discrete algorithms and methods for mobile computing and communications* (ACM, 1999), pp. 7–14.
 - [37] M. Molloy and B. Reed, *Random structures & algorithms* **6**, 161 (1995).
 - [38] G. Bianconi, *Physical Review E* **87**, 062806 (2013).
 - [39] G. J. Baxter, G. Bianconi, R. A. da Costa, S. N. Dorogovtsev, and J. F. Mendes, *Physical Review E* **94**, 012303 (2016).
 - [40] B. Min, S. Lee, K.-M. Lee, and K.-I. Goh, *Chaos, Solitons & Fractals* **72**, 49 (2015).
 - [41] D. Cellai, S. N. Dorogovtsev, and G. Bianconi, *Physical Review E* **94**, 032301 (2016).
 - [42] B. L. Chen, D. H. Hall, and D. B. Chklovskii, *Proceedings of the National Academy of Sciences of the United States of America* **103**, 4723 (2006).
 - [43] M. De Domenico, M. A. Porter, and A. Arenas, *Journal of Complex Networks* p. cnu038 (2014).

Supplemental Material

Message passing with edge overlap

This section is devoted to the description of the message-passing algorithm to approximate the behaviour of the Largest Mutually Observable Cluster (LMOC) in multiplex networks. The formalism differ from the one already presented in the main text for the fact that the only approximation used is the locally treelike ansatz. Edge overlap among layers is instead accounted by this framework. The method presented here is a generalization of the algorithm proposed in Ref. [28] for standard site percolation on multiplex networks. The method relies on the definition of the multilink $\vec{m}_{ji} = (a_{ji}^{[\alpha]}, a_{ji}^{[\beta]})$ for every pairs of nodes j and i in the duplex, where $a_{ji}^{[\alpha]} = 1$ if the nodes are connected in layer α , and $a_{ji}^{[\alpha]} = 0$, otherwise. The same definition applies for layer β . Messages considered in the approach are:

1. $u_{j \rightarrow i}^{\vec{m}_{ji}, \vec{n}}$, valid when node j is directly observable.
2. $v_{j \rightarrow i}^{\vec{m}_{ji}, \vec{n}}$, valid when node j is not directly observable.
3. $z_{j \rightarrow i}^{\vec{m}_{ji}, \vec{n}}$, valid when neither node i nor node j are directly observable.

In the definition of the messages, we use $\vec{n} = (n^{[\alpha]}, n^{[\beta]})$ to maintain the notation as compact as possible. Different message are indicated by different values of \vec{n} , namely $(0, 0)$, $(1, 0)$, $(0, 1)$, and $(1, 1)$. Note that if $n^{[\alpha]}(1 - a_{ji}^{[\alpha]}) + n^{[\beta]}(1 - a_{ji}^{[\beta]}) \neq 0$, the corresponding message is automatically zero. Further, normalization implies that $u_{j \rightarrow i}^{\vec{m}_{ji}, (0,0)} = 1 - u_{j \rightarrow i}^{\vec{m}_{ji}, (1,0)} - u_{j \rightarrow i}^{\vec{m}_{ji}, (0,1)} - u_{j \rightarrow i}^{\vec{m}_{ji}, (1,1)}$. It is further convenient to cumulate messages over layers as:

$$u_{j \rightarrow i}^{[\alpha]} = u_{j \rightarrow i}^{\vec{m}_{ji}, (1,0)} + u_{j \rightarrow i}^{\vec{m}_{ji}, (1,1)},$$

$$u_{j \rightarrow i}^{[\beta]} = u_{j \rightarrow i}^{\vec{m}_{ji}, (0,1)} + u_{j \rightarrow i}^{\vec{m}_{ji}, (1,1)},$$

and

$$u_{j \rightarrow i}^{[\alpha, \beta]} = u_{j \rightarrow i}^{\vec{m}_{ji}, (1,0)} + u_{j \rightarrow i}^{\vec{m}_{ji}, (0,1)} + u_{j \rightarrow i}^{\vec{m}_{ji}, (1,1)}.$$

The same definitions are valid for u - and z -type messages.

The probability that node i is in the LMOC is calculated in different manner depending on whether node i is (i) directly observable or (ii) not directly observable. For case (i), we have

$$q_i = \phi \left[1 - \left[\prod_{j \in \partial_i} (1 - \phi u_{j \rightarrow i}^{[\alpha]} - (1 - \phi) v_{j \rightarrow i}^{[\alpha]}) \right] - \left[\prod_{j \in \partial_i} (1 - \phi u_{j \rightarrow i}^{[\beta]} - (1 - \phi) v_{j \rightarrow i}^{[\beta]}) \right] + \left[\prod_{j \in \partial_i} (1 - \phi u_{j \rightarrow i}^{[\alpha, \beta]} - (1 - \phi) v_{j \rightarrow i}^{[\alpha, \beta]}) \right] \right]. \quad (\text{SM1})$$

Essentially, the probability for node i to be directly observable and part of the LMOC is given by the product of the probability to be directly observable and attached at least to another node that is part of the LMOC. The latter is estimated as one minus the probability that none of the nodes connected to i are part of the LMOC.

To account for the overlap among edges in the two layers, we need to make a distinction among neighbors of a node. We define three sets of neighbors for node i : $\partial_i^{[\alpha]}$, that is set of nodes that are neighbors of node i just in layer α ; $\partial_i^{[\beta]}$, that is set of nodes that are neighbors of node i just in layer β ; $\partial_i^{[\alpha, \beta]}$, that is the set of nodes that are neighbors of node i at the same time in both layers. In particular, we indicate with $k_i^{[\alpha]}$, $k_i^{[\beta]}$, $k_i^{[\alpha, \beta]}$ the size of the sets $\partial_i^{[\alpha]}$, $\partial_i^{[\beta]}$, $\partial_i^{[\alpha, \beta]}$, respectively. We also define degree of each node in layer α , layer β and total as follows: $k_i^{[1]} = k_i^{[\alpha]} + k_i^{[\alpha, \beta]}$, $k_i^{[2]} = k_i^{[\beta]} + k_i^{[\alpha, \beta]}$, $k_i^{[1,2]} = k_i^{[\alpha]} + k_i^{[\beta]} + k_i^{[\alpha, \beta]}$.

$$r_i = (1 - \phi) [1 - A - B + C] \quad (\text{SM2})$$

$$\begin{aligned}
A &= \left[\prod_{j \in \partial_i} (1 - \phi u_{j \rightarrow i}^{[\alpha]} - (1 - \phi) z_{j \rightarrow i}^{[\alpha]}) \right] + (1 - \phi)^{k_i^{[1]}} \left[1 - \prod_{j \in \partial_i} (1 - z_{j \rightarrow i}^{[\alpha]}) \right] \\
B &= \left[\prod_{j \in \partial_i} (1 - \phi u_{j \rightarrow i}^{[\beta]} - (1 - \phi) z_{j \rightarrow i}^{[\beta]}) \right] + (1 - \phi)^{k_i^{[2]}} \left[1 - \prod_{j \in \partial_i} (1 - z_{j \rightarrow i}^{[\beta]}) \right] \\
C &= \left[\prod_{j \in \partial_i} (1 - \phi u_{j \rightarrow i}^{[\alpha, \beta]} - (1 - \phi) z_{j \rightarrow i}^{[\alpha, \beta]}) \right] + (1 - \phi)^{k_i^{[1, 2]}} \left[1 - \prod_{j \in \partial_i} (1 - z_{j \rightarrow i}^{[\alpha, \beta]}) \right] + \\
&\quad \left[\prod_{j \in \partial_i^{[\alpha]}} (1 - \phi u_{j \rightarrow i}^{[\alpha]} - (1 - \phi) z_{j \rightarrow i}^{[\alpha]}) - (1 - \phi)^{k_i^{[\alpha]}} \prod_{j \in \partial_i^{[\alpha]}} (1 - z_{j \rightarrow i}^{[\alpha]}) \right] \times \\
&\quad (1 - \phi)^{k_i^{[2]}} \left[\prod_{j \in \partial_i^{[\alpha, \beta]}} (1 - z_{j \rightarrow i}^{[\alpha]}) - \prod_{j \in \partial_i^{[\beta]}} (1 - z_{j \rightarrow i}^{[\beta]}) \prod_{j \in \partial_i^{[\alpha, \beta]}} (1 - z_{j \rightarrow i}^{[\alpha, \beta]}) \right] + \\
&\quad \left[\prod_{j \in \partial_i^{[\beta]}} (1 - \phi u_{j \rightarrow i}^{[\beta]} - (1 - \phi) z_{j \rightarrow i}^{[\beta]}) - (1 - \phi)^{k_i^{[\beta]}} \prod_{j \in \partial_i^{[\beta]}} (1 - z_{j \rightarrow i}^{[\beta]}) \right] \times \\
&\quad (1 - \phi)^{k_i^{[1]}} \left[\prod_{j \in \partial_i^{[\alpha, \beta]}} (1 - z_{j \rightarrow i}^{[\beta]}) - \prod_{j \in \partial_i^{[\alpha]}} (1 - z_{j \rightarrow i}^{[\alpha]}) \prod_{j \in \partial_i^{[\alpha, \beta]}} (1 - z_{j \rightarrow i}^{[\alpha, \beta]}) \right] \tag{SM3}
\end{aligned}$$

The terms A and B are obvious. C instead contains a series of exceptions that must be handled to properly account for overlap. In particular,

1. The first term in C stands for the probability that node i is not connected to the LMOC in none of the layers. It accounts also for the exception where all of its neighbors are not directly observable.
2. Probability for node i of being not connected to LMOC through layer α and being not observable in layer β . Connections in layer β do not matter, but overlapping links, may connect node i to the LMOC in layer α .
3. Same as point 2, but swapping α with β .

The exceptions mentioned above are computed noting that

$$\begin{aligned}
\prod_{j \in \partial_i} (1 - \phi u_{j \rightarrow i}^{[\alpha, \beta]} - (1 - \phi) v_{j \rightarrow i}^{[\alpha, \beta]}) &= \left[\prod_{j \in \partial_i^{[\alpha]}} (1 - \phi u_{j \rightarrow i}^{(1, 0), (1, 0)} - (1 - \phi) v_{j \rightarrow i}^{(1, 0), (1, 0)}) \right] \times \\
&\quad \left[\prod_{j \in \partial_i^{[\beta]}} (1 - \phi u_{j \rightarrow i}^{(0, 1), (0, 1)} - (1 - \phi) v_{j \rightarrow i}^{(0, 1), (0, 1)}) \right] \times \\
&\quad \left[\prod_{j \in \partial_i^{[\alpha, \beta]}} (1 - \phi u_{j \rightarrow i}^{[\alpha, \beta]} - (1 - \phi) v_{j \rightarrow i}^{[\alpha, \beta]}) \right]. \tag{SM4}
\end{aligned}$$

We can now derive self-consistent equations for the messages. For u - and v -type messages, these are provided by the following equations:

$$\begin{aligned}
u_{j \rightarrow i}^{(1, 1), (1, 1)} = u_{j \rightarrow i}^{(1, 0), (1, 0)} = u_{j \rightarrow i}^{(0, 1), (0, 1)} &= 1 - \left[\prod_{k \in \partial_j \setminus i} (1 - \phi u_{k \rightarrow j}^{[\alpha]} - (1 - \phi) v_{k \rightarrow j}^{[\alpha]}) \right] \\
&\quad - \left[\prod_{k \in \partial_j \setminus i} (1 - \phi u_{k \rightarrow j}^{[\beta]} - (1 - \phi) v_{k \rightarrow j}^{[\beta]}) \right] + \left[\prod_{k \in \partial_j \setminus i} (1 - \phi u_{k \rightarrow j}^{[\alpha, \beta]} - (1 - \phi) v_{k \rightarrow j}^{[\alpha, \beta]}) \right], \tag{SM5}
\end{aligned}$$

$$u_{j \rightarrow i}^{(1, 1), (1, 0)} = \left[\prod_{k \in \partial_j \setminus i} (1 - \phi u_{k \rightarrow j}^{[\beta]} - (1 - \phi) v_{k \rightarrow j}^{[\beta]}) \right] - \left[\prod_{k \in \partial_j \setminus i} (1 - \phi u_{k \rightarrow j}^{[\alpha, \beta]} - (1 - \phi) v_{k \rightarrow j}^{[\alpha, \beta]}) \right], \tag{SM6}$$

$$u_{j \rightarrow i}^{(1,1),(0,1)} = \left[\prod_{k \in \partial_j \setminus i} (1 - \phi u_{k \rightarrow j}^{[\alpha]} - (1 - \phi) v_{k \rightarrow j}^{[\alpha]}) \right] - \left[\prod_{k \in \partial_j \setminus i} (1 - \phi u_{k \rightarrow j}^{[\alpha, \beta]} - (1 - \phi) v_{k \rightarrow j}^{[\alpha, \beta]}) \right], \quad (\text{SM7})$$

$$v_{j \rightarrow i}^{(1,1),(1,1)} = 1 - \left[\prod_{k \in \partial_j \setminus i} (1 - \phi u_{k \rightarrow j}^{[\alpha]} - (1 - \phi) z_{k \rightarrow j}^{[\alpha]}) \right] - \left[\prod_{k \in \partial_j \setminus i} (1 - \phi u_{k \rightarrow j}^{[\beta]} - (1 - \phi) z_{k \rightarrow j}^{[\beta]}) \right] + \left[\prod_{k \in \partial_j \setminus i} (1 - \phi u_{k \rightarrow j}^{[\alpha, \beta]} - (1 - \phi) z_{k \rightarrow j}^{[\alpha, \beta]}) \right], \quad (\text{SM8})$$

$$v_{j \rightarrow i}^{(1,1),(1,0)} = \left[\prod_{k \in \partial_j \setminus i} (1 - \phi u_{k \rightarrow j}^{[\beta]} - (1 - \phi) z_{k \rightarrow j}^{[\beta]}) \right] - \left[\prod_{k \in \partial_j \setminus i} (1 - \phi u_{k \rightarrow j}^{[\alpha, \beta]} - (1 - \phi) z_{k \rightarrow j}^{[\alpha, \beta]}) \right], \quad (\text{SM9})$$

$$v_{j \rightarrow i}^{(1,1),(0,1)} = \left[\prod_{k \in \partial_j \setminus i} (1 - \phi u_{k \rightarrow j}^{[\alpha]} - (1 - \phi) z_{k \rightarrow j}^{[\alpha]}) \right] - \left[\prod_{k \in \partial_j \setminus i} (1 - \phi u_{k \rightarrow j}^{[\alpha, \beta]} - (1 - \phi) z_{k \rightarrow j}^{[\alpha, \beta]}) \right], \quad (\text{SM10})$$

and

$$v_{j \rightarrow i}^{(1,0),(1,0)} = 1 - \left[\prod_{k \in \partial_j \setminus i} (1 - \phi u_{k \rightarrow j}^{[\alpha]} - (1 - \phi) z_{k \rightarrow j}^{[\alpha]}) \right] - \left[\prod_{k \in \partial_j \setminus i} (1 - \phi u_{k \rightarrow j}^{[\beta]} - (1 - \phi) z_{k \rightarrow j}^{[\beta]}) + (1 - \phi)^{k_j^{[2]}} \times \left[1 - \prod_{k \in \partial_j \setminus i} (1 - z_{k \rightarrow j}^{[\beta]}) \right] \right] + \left[\prod_{k \in \partial_j \setminus i} (1 - \phi u_{k \rightarrow j}^{[\alpha, \beta]} - (1 - \phi) z_{k \rightarrow j}^{[\alpha, \beta]}) + \left[\prod_{k \in \partial_j^{[\alpha]} \setminus i} (1 - \phi u_{k \rightarrow j}^{[\alpha]} - (1 - \phi) z_{k \rightarrow j}^{[\alpha]}) \times (1 - \phi)^{k_j^{[2]}} \times \left[\prod_{k \in \partial_j^{[\alpha, \beta]}} (1 - z_{k \rightarrow j}^{[\alpha]}) - \prod_{k \in \partial_j^{[\beta]}} (1 - z_{k \rightarrow j}^{[\beta]}) \prod_{k \in \partial_j^{[\alpha, \beta]}} (1 - z_{k \rightarrow j}^{[\alpha, \beta]}) \right] \right] \right]. \quad (\text{SM11})$$

For z -type message, the expressions are more complicated. We have that

$$\begin{aligned}
I &= \left[\prod_{k \in \partial_j \setminus i} (1 - \phi u_{k \rightarrow j}^{[\alpha]} - (1 - \phi) z_{k \rightarrow j}^{[\alpha]}) \right] + (1 - \phi)^{k_j^{[1]} - 1} \left[1 - \prod_{k \in \partial_j \setminus i} (1 - z_{k \rightarrow j}^{[\alpha]}) \right] \\
II &= \left[\prod_{k \in \partial_j \setminus i} (1 - \phi u_{k \rightarrow j}^{[\beta]} - (1 - \phi) z_{k \rightarrow j}^{[\beta]}) \right] + (1 - \phi)^{k_j^{[2]} - 1} \left[1 - \prod_{k \in \partial_j \setminus i} (1 - z_{j \rightarrow i}^{[\beta]}) \right] \\
(I, II) &= \left[\prod_{k \in \partial_j \setminus i} (1 - \phi u_{k \rightarrow j}^{[\alpha, \beta]} - (1 - \phi) z_{k \rightarrow j}^{[\alpha, \beta]}) \right] + (1 - \phi)^{k_j^{[1, 2]} - 1} \left[1 - \prod_{k \in \partial_j \setminus i} (1 - z_{j \rightarrow i}^{[\alpha, \beta]}) \right] + \\
&\quad \left[\prod_{k \in \partial_j^{[\alpha]}} (1 - \phi u_{k \rightarrow j}^{[\alpha]} - (1 - \phi) z_{k \rightarrow j}^{[\alpha]}) - (1 - \phi)^{k_j^{[\alpha]}} \prod_{k \in \partial_j^{[\alpha]}} (1 - z_{k \rightarrow j}^{[\alpha]}) \right] \times \\
&\quad (1 - \phi)^{k_j^{[2]} - 1} \left[\prod_{k \in \partial_j^{[\alpha, \beta]} \setminus i} (1 - z_{k \rightarrow j}^{[\alpha]}) - \prod_{k \in \partial_j^{[\beta]}} (1 - z_{k \rightarrow j}^{[\beta]}) \prod_{k \in \partial_j^{[\alpha, \beta]} \setminus i} (1 - z_{k \rightarrow j}^{[\alpha, \beta]}) \right] + \\
&\quad \left[\prod_{k \in \partial_j^{[\beta]}} (1 - \phi u_{k \rightarrow j}^{[\beta]} - (1 - \phi) z_{k \rightarrow j}^{[\beta]}) - (1 - \phi)^{k_j^{[\beta]}} \prod_{k \in \partial_j^{[\beta]}} (1 - z_{k \rightarrow j}^{[\beta]}) \right] \times \\
&\quad (1 - \phi)^{k_j^{[1]} - 1} \left[\prod_{k \in \partial_j^{[\alpha, \beta]} \setminus i} (1 - z_{k \rightarrow j}^{[\beta]}) - \prod_{k \in \partial_j^{[\alpha]}} (1 - z_{k \rightarrow j}^{[\alpha]}) \prod_{k \in \partial_j^{[\alpha, \beta]} \setminus i} (1 - z_{k \rightarrow j}^{[\alpha, \beta]}) \right] \tag{SM12}
\end{aligned}$$

$$\begin{aligned}
z_{j \rightarrow i}^{(1, 1), (1, 1)} &= 1 - I - II + (I, II) \\
z_{j \rightarrow i}^{(1, 1), (1, 0)} &= II - (I, II) \\
z_{j \rightarrow i}^{(1, 1), (0, 1)} &= I - (I, II) \tag{SM13}
\end{aligned}$$

$$\begin{aligned}
z_{j \rightarrow i}^{(1, 0), (1, 0)} &= 1 - \left[\prod_{k \in \partial_j \setminus i} (1 - \phi u_{k \rightarrow j}^{[\alpha]} - (1 - \phi) z_{k \rightarrow j}^{[\alpha]}) \right] + (1 - \phi)^{k_j^{[1]} - 1} \left[1 - \prod_{k \in \partial_j \setminus i} (1 - z_{k \rightarrow j}^{[\alpha]}) \right] - \\
&\quad \left[\prod_{k \in \partial_j \setminus i} (1 - \phi u_{k \rightarrow j}^{[\beta]} - (1 - \phi) z_{k \rightarrow j}^{[\beta]}) \right] + (1 - \phi)^{k_j^{[2]} - 1} \left[1 - \prod_{k \in \partial_j \setminus i} (1 - z_{j \rightarrow i}^{[\beta]}) \right] + \\
&\quad \left[\prod_{k \in \partial_j \setminus i} (1 - \phi u_{k \rightarrow j}^{[\alpha, \beta]} - (1 - \phi) z_{k \rightarrow j}^{[\alpha, \beta]}) \right] + (1 - \phi)^{k_j^{[1, 2]} - 1} \left[1 - \prod_{k \in \partial_j \setminus i} (1 - z_{j \rightarrow i}^{[\alpha, \beta]}) \right] + \\
&\quad \left[\prod_{k \in \partial_j^{[\alpha]} \setminus i} (1 - \phi u_{k \rightarrow j}^{[\alpha]} - (1 - \phi) z_{k \rightarrow j}^{[\alpha]}) - (1 - \phi)^{k_j^{[\alpha]} - 1} \prod_{k \in \partial_j^{[\alpha]} \setminus i} (1 - z_{k \rightarrow j}^{[\alpha]}) \right] \times \\
&\quad (1 - \phi)^{k_j^{[2]} - 1} \left[\prod_{k \in \partial_j^{[\alpha, \beta]}} (1 - z_{k \rightarrow j}^{[\alpha]}) - \prod_{k \in \partial_j^{[\beta]}} (1 - z_{k \rightarrow j}^{[\beta]}) \prod_{k \in \partial_j^{[\alpha, \beta]}} (1 - z_{k \rightarrow j}^{[\alpha, \beta]}) \right] + \\
&\quad \left[\prod_{k \in \partial_j^{[\beta]}} (1 - \phi u_{k \rightarrow j}^{[\beta]} - (1 - \phi) z_{k \rightarrow j}^{[\beta]}) - (1 - \phi)^{k_j^{[\beta]}} \prod_{k \in \partial_j^{[\beta]}} (1 - z_{k \rightarrow j}^{[\beta]}) \right] \times \\
&\quad (1 - \phi)^{k_j^{[1]} - 1} \left[\prod_{k \in \partial_j^{[\alpha, \beta]} \setminus i} (1 - z_{k \rightarrow j}^{[\beta]}) - \prod_{k \in \partial_j^{[\alpha]} \setminus i} (1 - z_{k \rightarrow j}^{[\alpha]}) \prod_{k \in \partial_j^{[\alpha, \beta]} \setminus i} (1 - z_{k \rightarrow j}^{[\alpha, \beta]}) \right] \tag{SM14}
\end{aligned}$$

$$\begin{aligned}
z_{j \rightarrow i}^{(0,1),(0,1)} = & 1 - \left[\prod_{k \in \partial_j \setminus i} (1 - \phi u_{k \rightarrow j}^{[\alpha]} - (1 - \phi) z_{k \rightarrow j}^{[\alpha]}) \right] + (1 - \phi)^{k_j^{[1]}} \left[1 - \prod_{k \in \partial_j \setminus i} (1 - z_{k \rightarrow j}^{[\alpha]}) \right] - \\
& \left[\prod_{k \in \partial_j \setminus i} (1 - \phi u_{k \rightarrow j}^{[\beta]} - (1 - \phi) z_{k \rightarrow j}^{[\beta]}) \right] + (1 - \phi)^{k_j^{[2]} - 1} \left[1 - \prod_{k \in \partial_j \setminus i} (1 - z_{j \rightarrow i}^{[\beta]}) \right] + \\
& \left[\prod_{k \in \partial_j \setminus i} (1 - \phi u_{k \rightarrow j}^{[\alpha, \beta]} - (1 - \phi) z_{k \rightarrow j}^{[\alpha, \beta]}) \right] + (1 - \phi)^{k_j^{[1,2]} - 1} \left[1 - \prod_{k \in \partial_j \setminus i} (1 - z_{j \rightarrow i}^{[\alpha, \beta]}) \right] + \\
& \left[\prod_{k \in \partial_j^{[\alpha]}} (1 - \phi u_{k \rightarrow j}^{[\alpha]} - (1 - \phi) z_{k \rightarrow j}^{[\alpha]}) - (1 - \phi)^{k_j^{[\alpha]}} \prod_{k \in \partial_j^{[\alpha]}} (1 - z_{k \rightarrow j}^{[\alpha]}) \right] \times \\
& (1 - \phi)^{k_j^{[2]} - 1} \left[\prod_{k \in \partial_j^{[\alpha, \beta]}} (1 - z_{k \rightarrow j}^{[\alpha]}) - \prod_{k \in \partial_j^{[\beta]} \setminus i} (1 - z_{k \rightarrow j}^{[\beta]}) \prod_{k \in \partial_j^{[\alpha, \beta]}} (1 - z_{k \rightarrow j}^{[\alpha, \beta]}) \right] + \\
& \left[\prod_{k \in \partial_j^{[\beta]} \setminus i} (1 - \phi u_{k \rightarrow j}^{[\beta]} - (1 - \phi) z_{k \rightarrow j}^{[\beta]}) - (1 - \phi)^{k_j^{[\beta]} - 1} \prod_{k \in \partial_j^{[\beta]} \setminus i} (1 - z_{k \rightarrow j}^{[\beta]}) \right] \times \\
& (1 - \phi)^{k_j^{[1]}} \left[\prod_{k \in \partial_j^{[\alpha, \beta]}} (1 - z_{k \rightarrow j}^{[\beta]}) - \prod_{k \in \partial_j^{[\alpha]}} (1 - z_{k \rightarrow j}^{[\beta]}) \prod_{k \in \partial_j^{[\alpha, \beta]}} (1 - z_{k \rightarrow j}^{[\alpha, \beta]}) \right]
\end{aligned} \tag{SM15}$$